Research Article

iMedPub Journals
www.imedpub.com

Nano Research & Applications
ISSN 2471-9838

2018
Vol.4 No.2:8

DOI: 10.21767/2471-9838.100037

Cerium Oxide Nanoparticle Attenuates Lipopolysaccharide (LPS) Induced Acute Kidney Injury (AKI) and Acute Lung Injury (ALI) in Male Sprague Dawley Rats

Kevin M Rice[1-4], Vellaisamy Selvaraj[1], Nandini DPK Manne[5], Ravikumar Arvapalli1, Michael Hambuchen[6], Eric R Blough[1,3,6,7] and Miaozong Wu[8]

1 Center for Diagnostic Nanosystems, Marshall University, Huntington, WV, USA
2 Department of Internal Medicine, Joan C. Edwards School of Medicine, Marshall University, Huntington, WV, USA
3 Biotechnology Graduate Program, West Virginia State University, Institute, WV
4 Department of Health and Human Service, School of Kinesiology, Marshall University, Huntington, WV
5 Department of Public Health, Marshall University, Huntington, WV, USA
6 Department of Pharmaceutical Sciences and Research, School of Pharmacy, Marshall University, Huntington, WV, USA
7 Department of Pharmacology, Physiology and Toxicology, Joan C. Edwards School of Medicine, Marshall University, Huntington, WV, USA
8 School of Geoscience, Physics, and Safety, College of Health, Science and Technology, University of Central Missouri

***Corresponding author:** Kevin M Rice

rice9@marshall.edu

Center for Diagnostic Nano systems Room 241D Robert C. Byrd Biotechnology Science Center, 1700 3rd Ave. Marshall University, Huntington, USA.

Tel: 304-638-2982
Fax: 304-696-3766

Citation: Rice KM, Selvaraj V, Manne NDPK, Arvapalli R, Hambuchen M (2018) Cerium Oxide Nanoparticle Attenuates Lipopolysaccharide (LPS) Induced Acute Kidney Injury (AKI) and Acute Lung Injury (ALI) in Male Sprague Dawley Rats. Nano Res Appl Vol.4 No.2:8

Abstract

Acute kidney injury (AKI) and lung injury (ALI) are a frequent and serious complication of sepsis that contributes significantly to mortality. This study aims to assess the capacity of cerium oxide nanoparticles (CeO_2 NP) to reduce lipopolysaccharide (LPS)-induced AKI and ALI in male Sprague Dawley rats. An intravenous dose of 0.5 mg/kg CeO_2 NP was administered at the onset of sepsis. This intervention significantly reduced tubular dilation, brush border loss, membrane regularity loss, and membrane damage. These changes were accompanied by diminished sepsis-induced increases in the kidney injury biomarkers, including blood urea nitrogen (BUN), creatinine, calbindin, kidney injury marker-1 (KIM-1), cystatin-C, and osteopontin. This attenuation of renal injury resulted in decreased oxidative stress, attenuated endoplasmic reticulum stress protein GRP-78 and eIF2-α induction, and reduced caspase-3 cleavage. In addition, CeO_2 NP improved lung structure, decreased myeloperoxidase activity, reduced oxidative stress, and diminished cytokine levels (TNF-α, IL-1β, IL-6). Based on these studies, CeO_2 NPs may be useful for the treatment of sepsis-related AKI and ALI, w_c=165

Keywords: Lipopolysaccharide (LPS); Sepsis; CeO_2 nanoparticles; Acute Kidney Injury (AKI); Acute Lung Injury (ALI)

Received: August 31, 2018; **Accepted:** October 03, 2018; **Published:** October 06, 2018

Introduction

Sepsis, the leading cause of mortality in critically ill patients, is characterized by multiple-organ dysfunction syndrome (MODS) [1,2]. Sepsis is known to impair both pulmonary and renal function, and the combination of acute lung injury (ALI) with acute kidney injury (AKI) from sepsis is associated with a >70% mortality rate % [2-4]. While the pathogenesis of sepsis has not yet been fully elucidated, it is understood the elevations of serum lipopolysaccharide (LPS) at least partly mediate the systemic inflammatory response syndrome (SIRS) that precedes the development of organ injury [4]. The development of SIRS is thought to be due, in large part, by the "over-activation" of the liver macrophages (Kupffer cells) which causes massive increases in the amount of circulating TNF-α, interleukin (IL)-1β, and IL-6 [5-11] which in turn are associated with increased renal and pulmonary oxidative stress and damage [12,13]. Because of the damaging effects that SIRS has on cellular ROS levels it has been postulated that anti-oxidant drugs may be effective in sepsis [14].

Recently, several nanoparticle compounds have been developed to scavenge reactive oxygen species (ROS) [15-18]. One compound that is potentially useful for biomedical applications is cerium oxide nanoparticles (CeO_2 NP) which may have efficacy in pathologies involving oxidative stress [18,19] and inflammation [20,21]. CeO_2 NPs are unique as they can effectively scavenge ROS by cycling between reduced (Ce^{+3}) and oxidized (Ce^{+4}) states [22]. In addition, CeO_2 NP act as superoxide dismutase [23] and catalase [24] mimetics depending on the particle redox state.

Current sepsis treatment is largely supportive in nature and is centered on the utilization of antibiotics, NSAIDS, intravenous fluids, and mechanical ventilator support where warranted [25]. Previously, our group showed that a single intravenous administration of 0.5 mg/kg CeO_2 NP significantly increased survival and reduced hepatic damage, serum cytokines and chemokines, and inflammatory related signaling in LPS-induced septic rats [26]. With the same animals and tissues utilized in our previous work [26], we hypothesized that a diminished SIRS response observed in these animals would result in decreased measurements of lung and kidney injury.

Material and Methods

CeO_2 NP preparation, characterization and administration

CeO_2 NP were acquired from Sigma (Manhattan, KS, USA) and prepared as described previously [26]. A Vibra Cell Sonicator (Sonics & Materials, Inc.) was used to prepare stock suspensions in dd H_20 (3.5 mg/ml, 2 min at 600 W, room temperature) prior to characterization. A Hitach-H-7000 electron microscope (50,000X magnification) was used for imaging. ImageJ software was used to calculate particle size. A particle size analyzer (HORIBA, Model-LB-550) equipped with a He-Ne laser (633 nm) determined the hydrodynamic size and size distribution of CeO_2 NP using back scattered light. Freshly prepared samples were analyzed in triplicate once daily over three days.

Animal care and experimental design

Male (300 - 350 g) Sprague-Dawley rats were purchased from Charles River Laboratories International Inc. Rats were dual housed with a 12/12- hr dark/light cycle at 22 ± 2˚C with *ad libitum* food and water. Rats acclimated for at least two weeks prior to experiments. All procedures were performed as described in the guide for the care and use of laboratory animals as approved by the council of the American Physiological Society and the institutional animal use review board of Marshall University. Rats were randomized into four groups: 1) The control group (n=6); 2) CeO_2 NPs group (n=6) that were administered 1.5 ml of endotoxin free water by the intraperitoneal (I.P.) route; 3) LPS (n=12) and 4) LPS + CeO_2 NP treatment groups were administered 1.5 ml of LPS (055-B5 from Sigma, 40 mg/kg) in sterile water by the I.P. route. Immediately after the injection of water or LPS, 200 µl of sterile distilled water was administered intravenously (tail vein) to the (1) control and (3) sepsis groups. Similarly, CeO_2 NP (0.5 mg/kg in 200 µl of sterile distilled water) was administered intravenously to the (2) CeO_2 NP and (4) sepsis + CeO_2 NP groups.

Tissue collection, estimation of CeO_2 NP content in kidney and lung and histology

Rats were humanely euthanized under anesthesia for collection of the kidneys and lungs at 6 or 24 hr after study initiation. Organs were cleaned with Krebs–Ringer bicarbonate buffer (KRB) to wash away any blood prior to flash freezing in liquid nitrogen and storage at -80˚C until analysis. CeO_2 NP content in organs was determined by Elemental Analysis Inc. (Lexington, KY) with induction coupled plasma-mass spectrometry (ICP-MS, described previously [27]). The kidney and lung were embedded in paraffin, and stained with hematoxylin and eosin (H&E) for histopathological analysis. Embedded samples were viewed using an EVOSfl fluorescence (Fisher Scientific, Pittsburgh, PA, USA). Another set of paraffin embedded kidney sample were stained with periodic acid Schiff (PAS) for the examination of basement membrane damage.

Evaluation of kidney damage markers and serum biochemical analysis

Blood, 6 or 24 h after the start of the study, was collected. It was then centrifuged (5,000xg for 10 min at room temperature) and stored as serum at -80˚C until analysis. Serum from each group (n=6) were pooled. Pooled serum was screened for biomarkers of kidney damage (β-2 microglobulin, calbindin, clusterin, cystatin-C, epidermal growth factor rat (EGF-Rat), kidney injury molecule-1 (KIM-1), neutrophil gelatinase-associated lipocalin (NAGL), osteopontin, tissue inhibitory of metalloproteinase-1 (TIMP-1), and vascular endothelial growth factor A (VEGF-A)) and renal function (cystatin-C)) by Myriad RBM (Austin, TX) in triplicate. An Abaxis VetScan® analyzer (Abaxis, Union City, CA, USA) was used to quantitate serum levels of BUN, creatinine and potassium.

Assessment of apoptosis in kidney by TUNEL staining

Sections of paraffin embedded tissue (5 µm, prepared as per manufacturer's specifications) were analyzed with a TUNEL staining kit (Roche Applied Science, Indianapolis, IN). As a positive control, identical experiments were performed with DNase I. Experiments omitting the labeling reagent were used as a negative control. An EVOSfl fluorescence microscope (Fisher Scientific, Pittsburgh, PA, USA, 200x magnification) was used to capture images for counting of TUNEL-positive nuclei. Data was reported as the number of TUNEL-positive nuclei/500 nuclei.

Renal and lung superoxide level assessment

Superoxide levels in the renal and lung sections were estimated using dihydroethidium staining after deparafinization and rehydration of tissue sections. This involved room temperature incubation of sections with 5 mM dihydroethidium for 1 h in a dark room. An Evos FL microscope (Life technologies, Grand Island, NY) was used to image each section after it was washed with PBS (3 × 5 min). Mean fluorescence intensity was determined across various groups using image J analysis software as a measure for superoxide levels.

SDS-PAGE and immunoblotting

Sections of frozen kidney and lung (~100 mg) were pulverized to a fine powder. The powder was then added to 900 µl of T-PER (Pierce, Rockford, IL, USA) which contained 1% protease and phosphatase inhibitors. The organ mixture was then homogenized prior to centrifugation (10,000×g for 10 min, 4°C) and the supernatant was collected. The protein in each sample was quantified by a 660 nm protein assay (Pierce, Rockford, IL, USA). Each sample was identically diluted with Laemilli buffer (4x) and loaded onto a 10% PAGEr Gold Tris-Glycine Precast gel (Lonza, Rockland, ME), subjected to SDS-PAGE, and then transferred to a nitrocellulose membrane as previously described [28]. Milk (5%) in TBST was used as a blocking agent and incubated with the membrane for 1 h and prior to probing with the proper primary antibody (Cell Signaling Technology, Danvers, MA). Afterward, TBST was used to wash the membranes (3 × 5 min) before 1 h of incubation with secondary antibody (anti-rabbit, Cell Signaling Technology, Danvers, MA). Super-signal West Pico Chemiluminiscent substrate (Pierce, Rockford, IL, USA) was used to determine immunoreactivity and Fluorchem 9900 software (Protein Simple, Santa Clara, CA) was used to quantitate this property.

Measurement of inflammatory cytokines and chemokines in lung homogenate

The relative concentrations of 12 proinflammatory cytokines/chemokines in the lung tissue lysate (n = 6/group at 6 h and 24 h) were determined with a Rat Inflammatory Cytokines Multi-Analyte ELISArray kit (Qiagen, CA, USA, catalogue number MER004A) as suggested by the manufacturer.

Myeloperoxidase activity (MPO) in lung homogenate

Myeloperoxidase activity, a general peroxidase activity, was performed as previously described [29]. Frozen lung samples were homogenized and sonicated in 50 mmol/l potassium phosphate buffer containing 0.5% hexadecyltrimethyammonium bromide (HTAB) and 5 mmol/l ethylene diamine tetracetic acid (EDTA). Afterward, these samples were centrifuged (10000xg for 10 min, 4°C) prior to the collection of the supernatant. Supernants were incubated in a 50 mmol/l potassium phosphate buffer containing H_2O_2 (1.5 mol/l) and O-dianisidine dihydrochloride (167 µg/ml). The enzyme activity was determined spectrophotometically by measuring the change in absorbance at 460 nm over 3 minutes in a 96-well plate reader. Values represent the change in OD/min/gram tissue weight.

Statistical analysis

Data from these studies was reported as mean ± standard error of the mean (SEM). A one way ANOVA was performed in SigmaStat (Aspire Software International, Auburn VA) to analyze dependent variables; *post-hoc* tests were performed when appropriate. Significance was set at $p<0.05$.

Results

Characterization of CeO_2 NP

Scanning electron microscopy (SEM, **Figure 1**) and transmission electron microscopy **(Figure 1)** analysis estimated each nanoparticle to be approximately 40 - 60 nm long. Experiments using dynamic light scattering were used to estimate CeO_2 NP mean hydrodynamic diameter to be approximately 63 ± 11 nm **(Figure 1)**.

CeO_2 NP administration provided protection against renal damage

Kidney ceria content was not increased by nanoparticle treatment relative to untreated animals **(Table 1)**. The LPS treatment decreased kidney weight while the CeO_2 NP treatment was increased kidney weight (**Table 1**, *p<0.05*).

Compared to control animals, serum blood urea nitrogen (BUN) and creatinine (SCr) levels were significantly higher at 6 and 24 h in the septic animals (*p<0.05*). The amount of serum phosphorus was lower at 6 h in septic animals (*p<0.05*). CeO_2 nanoparticle treatment decreased BUN and creatinine (SCr) at 24 h and increase the serum phosphorus level at 6 h (**Figure 1,** *p<0.05*). In the H & E kidney tissue in the sepsis group, there was structural deterioration of the glomerulus, decreased Bowman's space, loss of brush border, and tubular cell sloughing **(Figure 1)**. Similarly, as seen in the PAS stained kidney tissue, sepsis was also linked to the loss of brush border and thickening of the parietal Bowman's capsule **(Figure 1)**. CeO_2 nanoparticle treatment appeared to attenuate the deleterious effects of sepsis on renal structure **(Figure 1)**.

CeO_2 NP attenuate sepsis induced biomarkers for the early detection of AKI

Sepsis elevated the levels of β-2 microglobulin, osteopontin, NAGA, VEGT-A and TIMP-1 rat at 6 h, and calbindin, β-2 microglobulin, KIM-1 rat, cystatin-C, osteopontin, NGAL, VEGT-A and TIMP-1 rat at 24 h time points relative to control animals. Treatment with CeO_2 nanoparticles attenuated sepsis induced increases in calbindin, KIM-1 rat, cystatin-C and osteopontin at 24 h (**Figure 2**, *p<0.05*).

CeO_2 NP attenuate sepsis induced oxidative stress and renal apoptosis

Relative to controls, animals in the septic group appeared to exhibit increased superoxide levels. CeO_2 NP treatment, however, resulted in decreased superoxide levels **(Figure 3)**. Similarly, sepsis associated increases in GRP-78, phosphorylated elf-2, and HSP-90 were decreased with CeO_2 nanoparticles treatment (**Figure 3**, (*p<0.05*)).

The TUNEL staining procedure was employed to quantitate the number of nuclei containing fragmented DNA. This analysis was used to determine if kidney damage was associated with elevated cellular apoptosis. It was found that sepsis resulted in an increase in the count of TUNEL positive nuclei relative to control, but nanoparticle treatment resulted in a reduction in these counts relative to control (**Figure 4**, $p<0.05$). Consistent with these data, sepsis-induced increases in cleaved caspase-3 (19 and 17-kDa fragment) and the Bax/Bcl-2 ratio were also decreased following nanoparticle treatment (**Figure 4**, *p<0.05*).

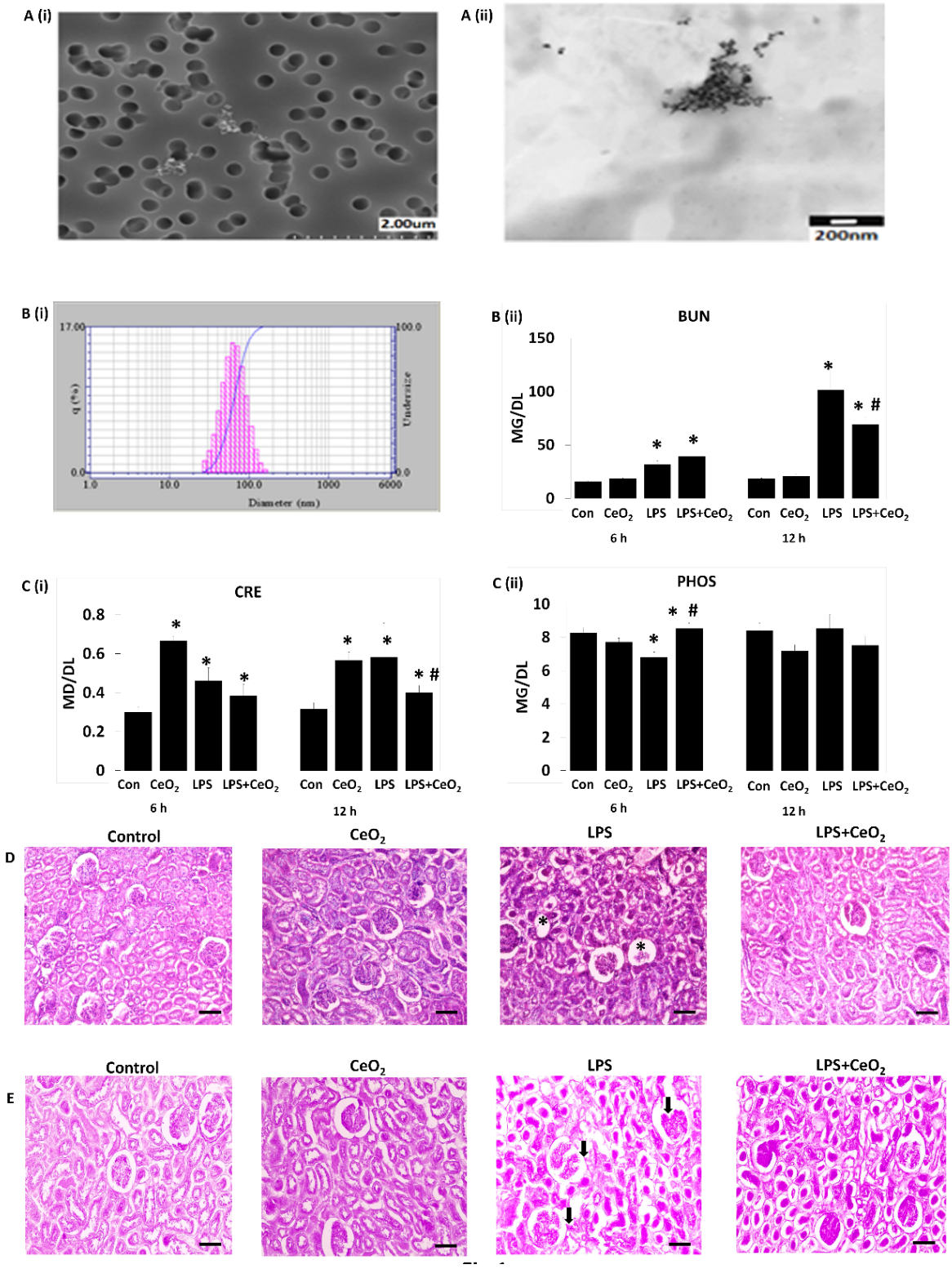

Figure 1 CeO_2 NP characterization and the effect of the agent on LPS- induced acute kidney injury. A (i) SEM image of CeO_2 NP, A (ii) TEM image of CeO_2 NP, B (i) Dynamic light scattering (DLS) size histogram, B (ii) blood urea nitrogen (BUN) level in serum, C (i) creatinine level in serum, C (ii) phosphorous level in serum (n=6/group). Values are mean ± SEM (≥ 3 independent analyses). Representative micrographs of kidney tissue (n=3/group) 24 h after sepsis induction as visualized by light microscopy, (D) visual inspection of the kidney sections by H & E staining demonstrated evidence of increased Bowman's space (*) and renal tubular necrosis, (E) PAS staining showed the basal membrane damage and irregularities. *p<0.05 compared to the control group, # p<0.05 compared to LPS group.

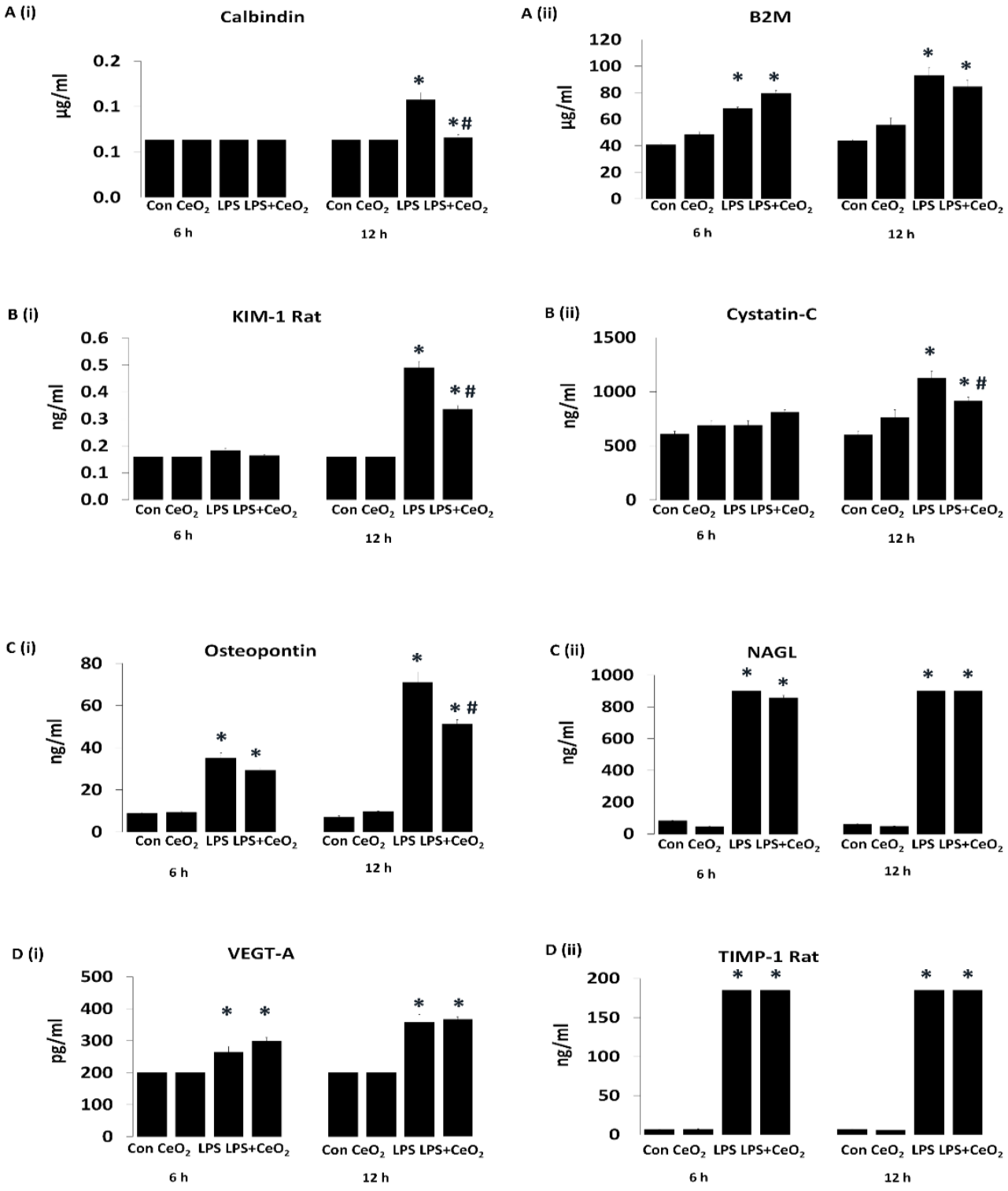

Fig-2

Figure 2 CeO_2 NP effect on LPS-induced elevations in biomarkers of AKI. Markers: A (i) calbindin, A (ii) β-2 microglobulin, B (i) kidney injury molecule-1 (KIM-1), B (ii) cystatin-C, C (i) osteopontin, C (ii) neutrophil gelatinase-associated lipocalin (NAGL), D (i) vascular endothelial growth factor-A (VEGF-A) and D (ii) tissue inhibitory of metalloproteinase-1 (TIMP-1). Values are mean ± SEM of at least three independent experiments. *p<0.05 compared to control group, # p<0.05 compared to LPS group.

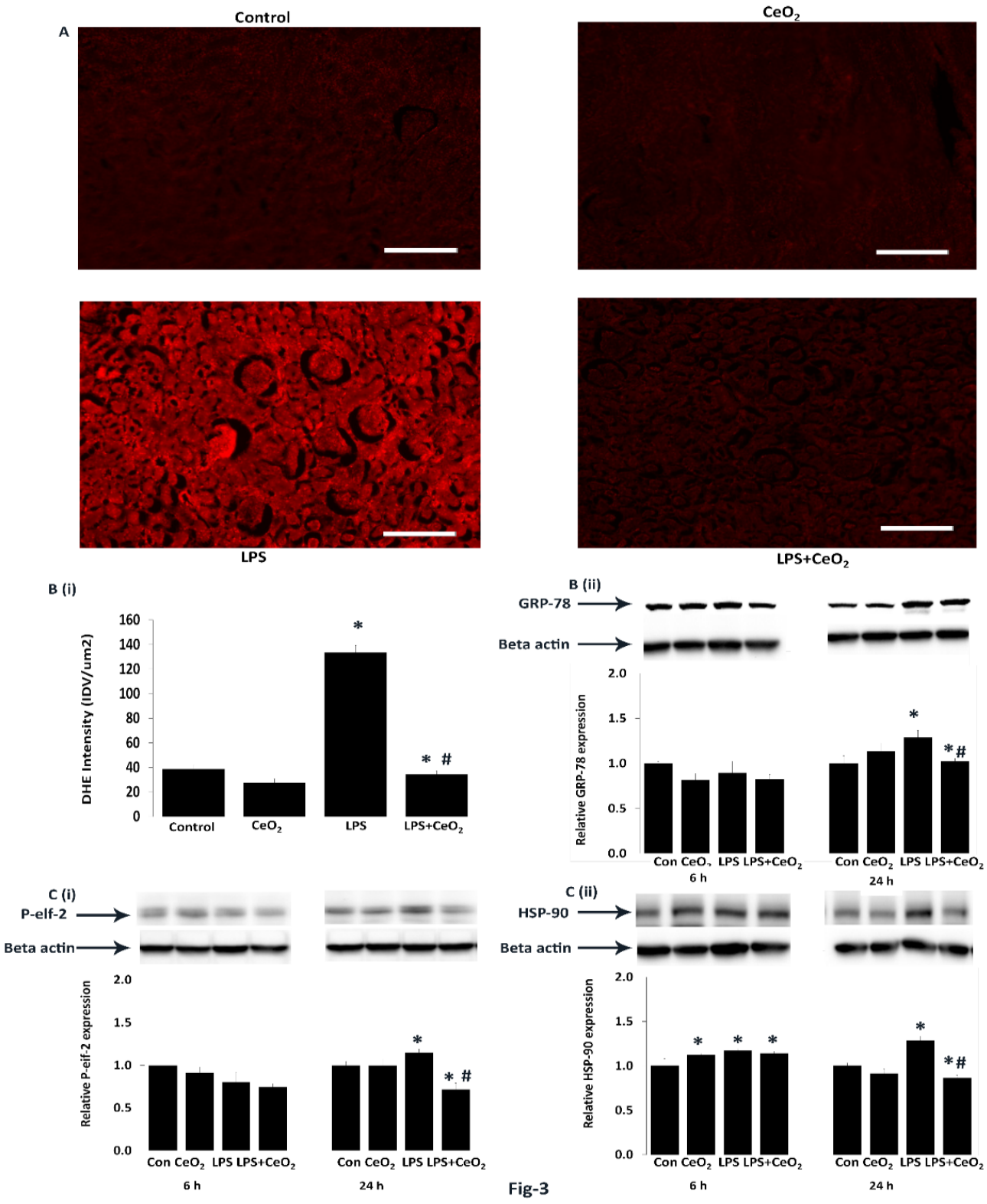

Figure 3 CeO_2 NP effects on LPS induced renal superoxide level and inflammatory markers. Representative images of kidney tissue (n=3/group) stained with dihydroethidium (DHE) 24 h after sepsis induction as visualized by fluorescent microscopy and imaged at 200x (Scale bar=100 µm). B (i) Quantification of superoxide levels indifferent groups. Both total and phosphorylated proteins were quantitated by immunoblotting and normalized to GAPDH, B (ii) GRP-78, C (i) p-elF-2, and C (ii) HSP-90. Values are mean ± SEM of at least three independent experiments. *p<0.05 compared to control group, # p<0.05 compared to sepsis group.

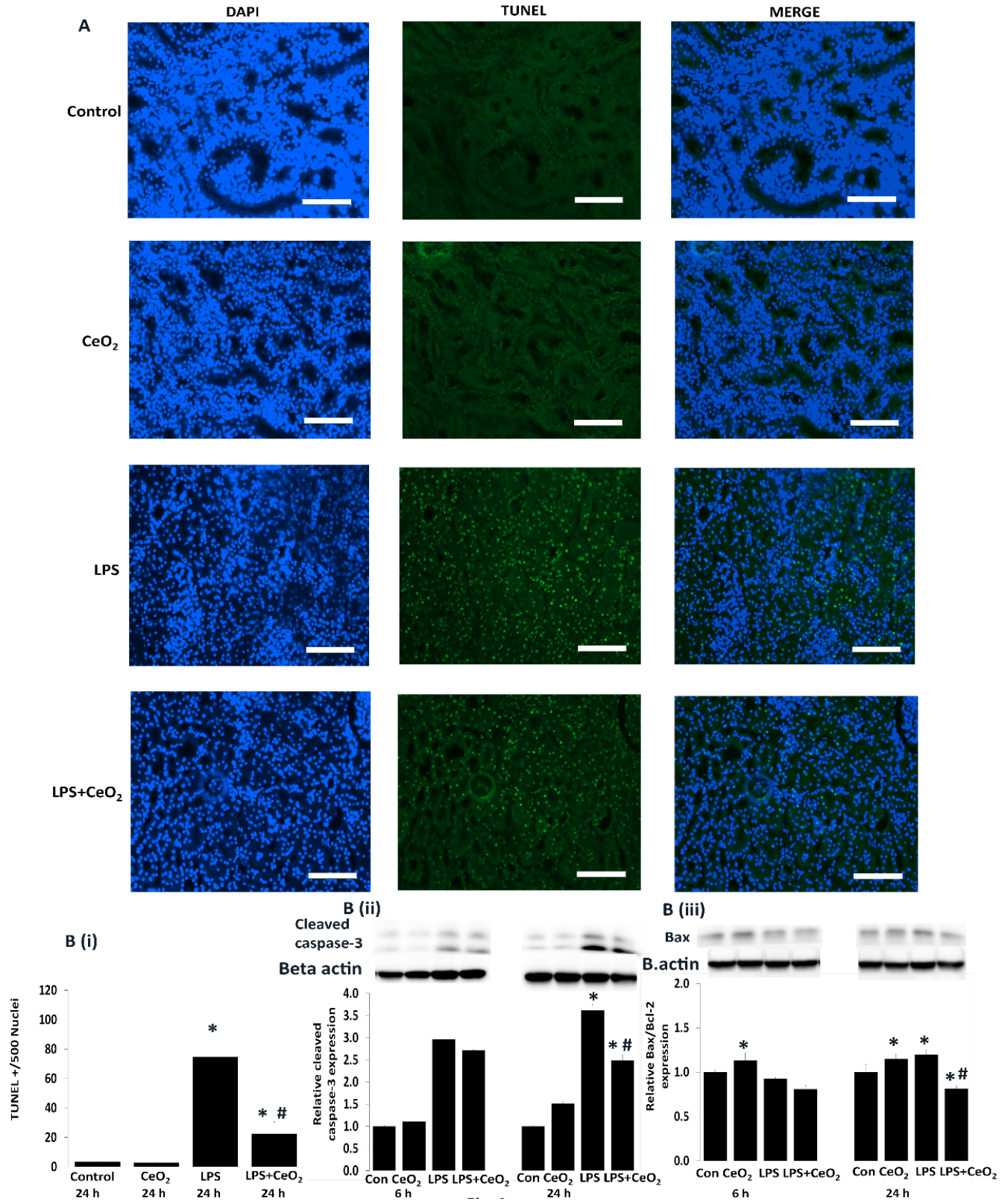

Figure 4 Effect of CeO_2 NP on apoptosis and its marker proteins changes induced by LPS. A. Mitochondrial dependent renal apoptosis was measured by a TUNEL method (n=3 scale bar=100 µm), B (i) measurement of TUNEL positive nuclei. Western blotting (normalized to GAPDH) was used to measure apoptotic mediator protein expression levels: B (ii) cleaved caspase-3, and B (iii) Bax/Bcl-2 ratio. Values are mean ± SEM of at least three independent experiments. *P <0.05 compared to control group, # p<0.05 compared to sepsis group.

CeO_2 NP administration increases lung ceria content and decreases lung damage

Relative to untreated control rats, lung ceria content was elevated in animals receiving nanoparticle injections **(Table 1)**. Sepsis increased and nanoparticle treatment decreased lung weight **(Table 1)**, *p<0.05*). in the control and cerium oxide groups, the lung morphology was unremarkable **(Figure 5)**. In contrast, lung tissues from septic animals exhibited extensive morphological damage, including evidence of hemorrhage, interstitial edema, thickening of the alveolar wall, and increased tissue infiltration with leukocytes **(Figure 5)**. As with lung weight, we found that

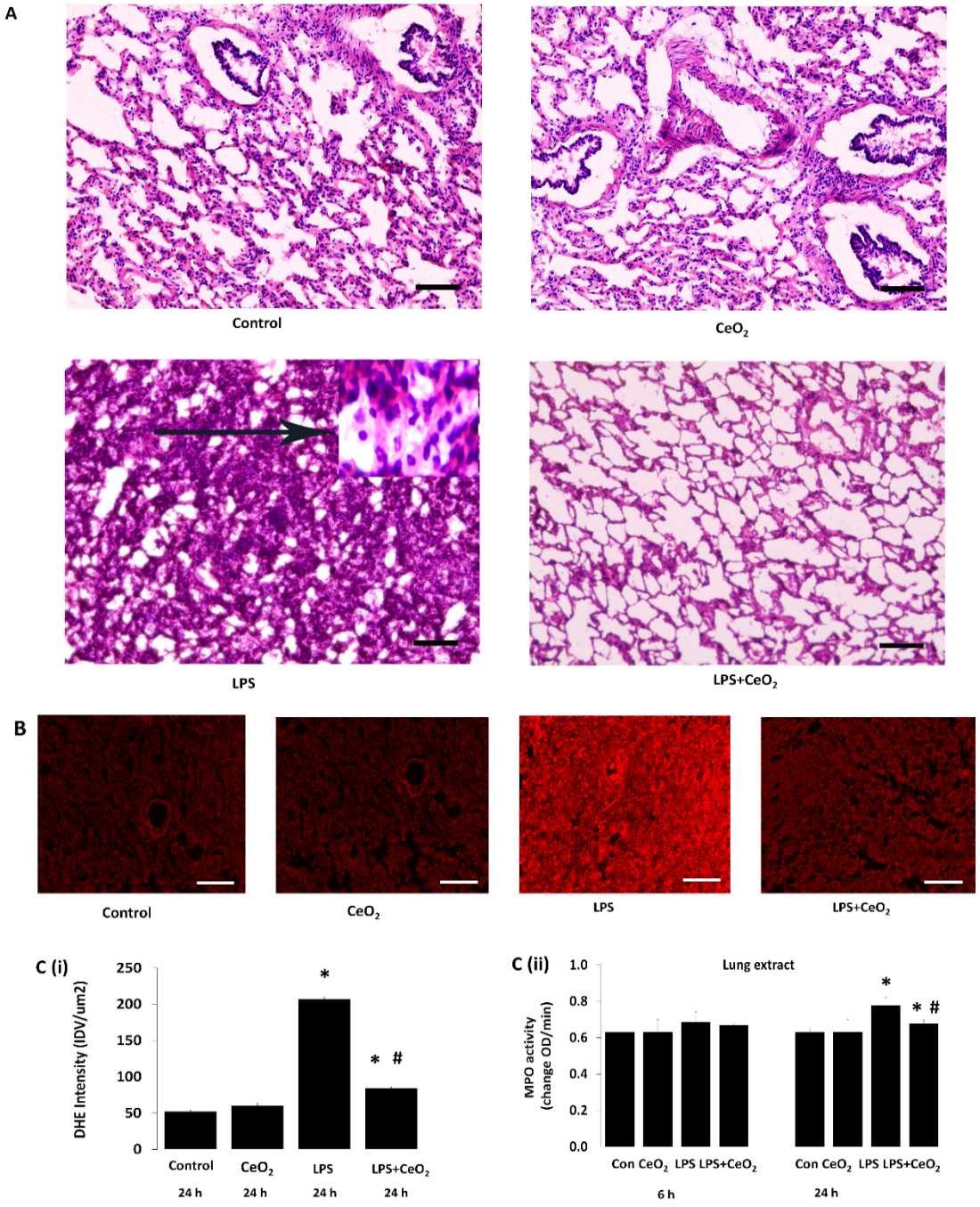

Figure 5 Effect of CeO_2 NP on sepsis- induced lung injury and superoxide level and MPO activity. A. Representative images of lung morphology (n=3/group) 24 h after sepsis induction as visualized by light microscopy. Septic related changes in the lung were associated with changes in alveolar structure, evidence of pulmonary inflammation, neutrophil infiltration and a thickening of the alveolar septum. B. Representative micrographs of lung tissue (n=3/group) stained with dihydroethidium (DHE) 24 h after sepsis induction and visualized by fluorescent microscopy and imaged at 200 X (Scale bar=100 µm). C (i) Superoxide quantification by group. C (ii) levels of myeloperoxidase activity in lung homogenate from control (n=6), CeO_2NP (n=6), sepsis (n=6), sepsis+CeO_2 NP (n=6): analyzed in triplicate. *Significantly different from control (P < 0.05). # Significantly different from LPS treatment (P < 0.05).

Table 1 Cerium oxide accumulation in different organs and their weight.

Different Organ & Experimental Group	CeO_2 concentration (ppm)		Organ weight (g)	
	6 h	24 h	6 h	24 h
Organ	Kidney			
Control	<0.120 ± 0.0057	<0.123 ± 0.0088	1.397 ± 0.061	1.421 ± 0.021
CeO_2	<0.113 ± 0.0090	<0.110 ± 0.0057	1.420 ± 0.058	1.421 ± 0.050
LPS	Not tested	Not tested	1.408 ± 0.069	1.394 ± 0.022*
LPS+CeO_2	<0.11 ± 0.0033	<0.136 ± 0.0236	1.420 ± 0.058	1.421 ± 0.072*#
Organ	Lungs			
Control	<0.120 ± 0.0057	<0.120 ± 0.0057	1.433 ± 0.048	1.408 ± 0.042
CeO_2	<0.120 ± 0.0057	0.80 ± 0.0493*	1.428 ± 0.062	1.408 ± 0.021
LPS	Not tested	Not tested	1.490 ± 0.040	1.856 ± 0.061*
LPS+CeO_2	<0.120 ± 0.0057	0.68 ± 0.2150*	1.428 ± 0.021	1.408 ± 0.021*#

Kidney and lung samples from each of the different groups (n=6/group). Values are mean ± SEM of at least 3 independent experiments performed in triplicate. Statistical significance was determined by a one way ANOVA. Asterisks indicate *significantly different from control group, *#significantly difference from sepsis group ($p<0.05$).

CeO_2 np administration prevented the occurrence of visible sepsis related lung injury **(Figure 5)**.

CeO_2 NP attenuate sepsis induced increases in MPO activity and inflammatory signaling in the lungs

Infiltration of neutrophils into the lung is an important feature of LPS-induced ALI [30]. To evaluate the effects of the CeO_2 nanoparticle treatment on lung neutrophil levels, we determined the effect of sepsis and CeO_2 NP treatment on lung MPO activity. Consistent with our histological data, sepsis increased and the nanoparticle treatment decreased MPO activity (**Figure 5**, *p<0.05*). Similarly, lung sections collected from septic animals exhibited increased in superoxide levels compared to control rats (**Figure 5**, *p<0.05*). The superoxide levels were decreased by CeO_2 NP administration (**Figure 5**, *p<0.05*). Compared to control animals, sepsis increased and the nanoparticle treatment decreased the expression of TNF-α, IL-6, IL-1α and IL-1β (**Figure 6**, *p<0.05*). Following the lung histology, sepsis increased the amount of phosphorylated ERK1/2 and Bax, while CeO_2 NP administration decreased these measurements **(Figure 6)**.

Discussion

Sepsis induced AKI and ALI are two common side effects of sepsis which are associated with increased patient morbidity and mortality [31,32]. The standard treatment for AKI and ALI is primarily supportive in nature [2,33]. Herein, we examine if CeO_2 NP are effective in protecting the kidney and lung following a sepsis. As found previously, sepsis was associated with both AKI and ALI **(Figures 1-5)**. In the renal studies, sepsis resulted in increased serum blood urea nitrogen, creatinine along with several biomarkers of renal injury including KIM-1 and β-2 microglobulin **(Figure 1)**. From a functional perspective, we also found that sepsis appeared to decrease the renal glomerular filtration rate as evidence by increased serum cystatin-C levels [34]. Importantly, we found that these changes were attenuated with a one-time administration of the CeO_2 NP **(Figure 2)**.

It is thought that the increased oxidative stress caused by SIRS is one of the primary causes of sepsis associated organ damage [35]. Recent data suggests that CeO_2 NP can function as highly active ROS scavengers in addition to acting as catalase and SOD mimetics [36]. As predicted, in the current study CeO_2 NP treatment significantly reduced sepsis-induced increases in renal superoxide oxide measurements **(Figure 3)**. In addition to increased ROS, elevations in ER stress have also been suggested in the pathogenesis of acute kidney diseases [37]. To examine this, we next determined how sepsis and the nanoparticle treatment affected the expression of the ER stress makers, GRP-78 and eIF2α. Relative to control animals, the GRP-78 and eIF2α expression was significantly elevated with sepsis and importantly, attenuated by the CeO_2 NP treatment **(Figure 3)**.

In addition to increases in cellular ROS and ER stress, it is also posited that renal cell apoptosis may also play a role in AKI [38]. To investigate this, we tested the effectiveness of CeO_2 NP in reducing cellular apoptosis in the kidney. As per our histological analysis and measurement of renal damage, we found that sepsis increased the counts of TUNEL positive cells, elevated the amount of cleaved caspase-3, and increased the Bax/Bcl-2 ratio which was reduced by CeO_2 NP administration **(Figure 4)**.

Sepsis-induced acute lung injury (ALI) in animals is characteristic of excessive infiltration of neutrophils, pro-inflammatory cytokine release, and loss of vascular barrier integrity [39]. It is thought that activated neutrophils can induce the extensive lung inflammation that oftentimes increases the permeability of alveolar capillary membrane [40]. Indeed, migrating neutrophils cause mechanical damage to alveolar structure and worsen the influx of fluid into alveolar space [41]. In addition, neutrophils can also release free radicals that cause oxidative stress which play an important role in structural, functional and inflammatory responses that characterized ALI [42]. In the current study, LPS resulted in significant alteration in the pulmonary structure that was accompanied by neutrophil infiltration in the lung interstitial space and enhanced MPO activity **(Figure 5)**. Similar to the kidneys, the CeO_2 NP reduced visible lung injury relative to control **(Figure 5)**.

Inflammatory cytokines are believed to be crucially involved in the lung injury/damage in observed in septic animals. Among these cytokines, TNF-α, IL-1β and IL-6 are thought to play critical roles

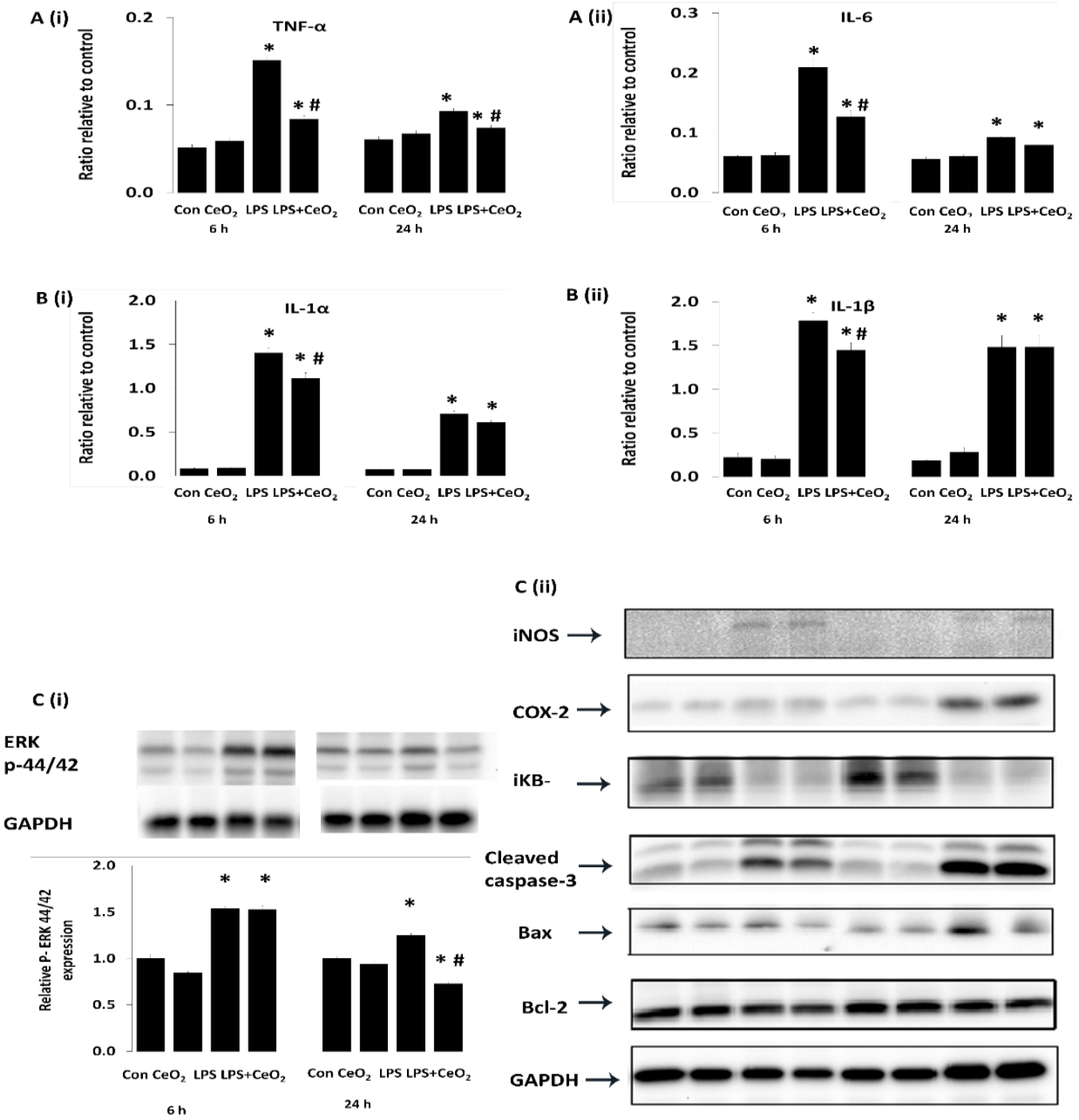

Figure 6 Protective effect of CeO_2 NP on LPS induced cytokines and apoptotic related markers. Cytokines and chemokine levels were determined in lung homogenates: A (i) TNF-α, A (ii) IL-6, B (i) IL-1 α, and B (ii) IL-1β. Homogenates were pooled in control (n=6), CeO_2 NP (n=6), Sepsis (n=6), Sepsis+CeO_2NP (n=6). Pooled homogenate was analyzed in triplicate. C (i) ERK-P-44/42 marker protein, C (ii) apoptotic and inflammatory related marker proteins were determined by immunoblotting. *Significantly different from control ($P < 0.05$). #Significantly different from LPS treatment ($P < 0.05$).

in early phase of ALI. It has been reported that resident alveolar macrophages and recruited neutrophils release TNF-α and IL-1β in early phase of inflammation in response to the pathogen stimulus, resulting in the subsequent inflammatory cascade and

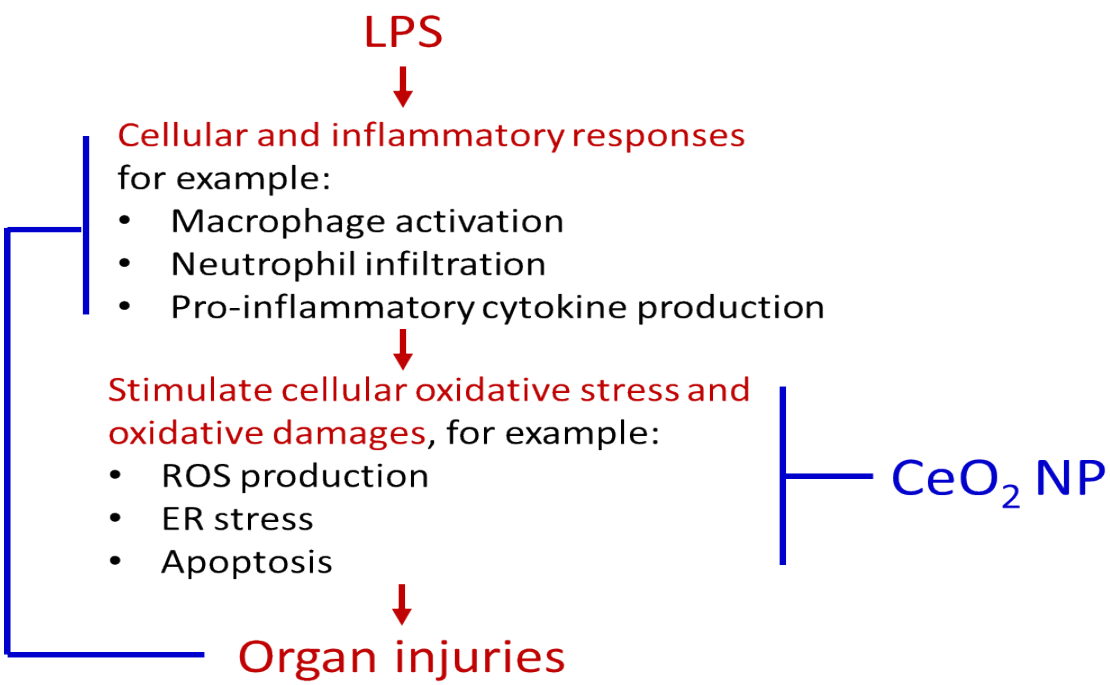

Figure 7 Proposed mechanism of CeO_2 NP in attenuation of acute kidney injury (AKI) and acute lung injury (ALI). Lipopolysaccharide (LPS) can trigger cellular and inflammatory responses, which result in tissue excessive oxidative stress and organ injuries. CeO_2 NP exerts protective effects, at least in part, by attenuating oxidative stress and damages. Red arrow indicates "triggering/stimulating/increasing", and blue line suggests "inhibiting/decreasing".

lung injury [43]. In the current study, the expression of TNF-α, IL-1β, IL-1α and IL-6 were markedly induced by LPS challenge, which was blocked by CeO_2 NP administration **(Figure 6)**.

In addition to elevation in cytokine concentrations, excessive iNOS and COX-2 expression may contribute to the pathophysiology of sepsis-induced ALI [44]. In the current study, it was found that LPS increased iNOS and COX-2 expression in lung homogenates, while CeO_2 NP treatment decreased iNOS and COX-2 protein levels. As with the renal studies, and consistent with our histological analysis, we also found that CeO_2 NP can attenuate LPS-induced elevations in the Bax/Bcl-2 ratio and caspase-3 cleavage **(Figure 4)**.

Conclusion

In summary, this study demonstrated that a single dose 0.5 mg/kg of intravenous CeO_2 NP to rats with LPS-induced sepsis significantly decreased the severity of AKI and ALI. In addition to improvements in renal structure, the CeO_2 NP treatment also decreased circulating NGAL and Kim-1 levels, ER stress and renal apoptosis. Similarly, the CeO_2 NP also resulted in improved in lung morphology, and decreased neutrophil infiltration, MPO activity, and pulmonary cytokine expression (TNF-α, IL-1β, IL-6). Therefore, we propose that CeO_2 NP acts on reducing sepsis-induced oxidative stress, and hence exerts a protective effect on acute kidney and lung injuries **(Figure 7)**. However, much in-depth work remains. For example, how CeO_2 NP can diminish pulmonary neutrophil infiltration? How CeO_2 NP can change critical biomarkers (such as HSP-90, eIF2α, GRP-78, caspase-3, and Bax) in terms of translational or post-translational mechanisms? With more thorough investigations, we will be able to understand better the mechanism of CeO_2 NP protective effects in sepsis as a whole. Based on our current data, CeO_2 NP could be a potential pharmacotherapy for sepsis-associated AKI and ALI.

Acknowledgements

This work was supported in part from DOE grant (DE-PS02-09ER-01 to E.R.B).

References

1 Angus DC, Linde-Zwirble WT, Lidicker J, Clermont G, Carcillo J, et al. (2001) Epidemiology of severe sepsis in the United States: analysis of incidence, outcome, and associated costs of care Crit Care Med 29: 1303-1010.

2 Ogura T, Nakamura Y, Takahashi K, Nishida K, Kobashi D, et al. (2018) Treatment of patients with sepsis in a closed intensive care unit is associated with improved survival: a nationwide observational study in Japan. J Intensive Care 6: 57.

3 Bagshaw SM, Uchino S, Bellomo R, Morimatsu H, Morgera S, et al. (2007) Septic acute kidney injury in critically ill patients: clinical characteristics and outcomes. Clin J Am Soc Nephrol 2: 431-439.

4 Heemskerk S, Masereeuw R, Russel FG, Pickkers P (2009) Selective

iNOS inhibition for the treatment of sepsis-induced acute kidney injury. Nat Rev Nephrol 5(11): 629-640.

5 Niesler U, Palmer A, Fröba JS, Braumüller ST, Zhou S, et al. (2014) Role of alveolar macrophages in the regulation of local and systemic inflammation after lung contusion. J Trauma Acute Care Surg 76(2): 386-393.

6 Neunaber C, Oestern S, Andruszkow H, Zeckey C, Mommsen P, et al. (2013) Cytokine productive capacity of alveolar macrophages and Kupffer cells after femoral fracture and blunt chest trauma in a murine trauma model. Immunol Lett 152: 159-166.

7 Seitz DH, Perl M, Liener UC, Tauchmann B, Braumüller ST, et al. (2011) Inflammatory alterations in a novel combination model of blunt chest trauma and hemorrhagic shock J Trauma 70: 189-96.

8 Lee SH, Clemens MG, Lee SM (2010) Role of Kupffer cells in vascular stress genes during trauma and sepsis. J Surg Res 158: 104-111.

9 Campbell SJ, Zahid I, Losey P, Law S, Jiang Y, et al. (2008) Liver Kupffer cells control the magnitude of the inflammatory response in the injured brain and spinal cord. Neuropharmacology 55: 780-7.

10 Gong JP, Wu CX, Liu CA, Li SW, Shi YJ, et al. (2002) Intestinal damage mediated by Kupffer cells in rats with endotoxemia. World J Gastroenterol 8: 923-937.

11 Koo DJ, Chaudry IH, Wang P (1999) Kupffer cells are responsible for producing inflammatory cytokines and hepatocellular dysfunction during early sepsis. J Surg Res 83: 151-157.

12 Kovtunovych G, Ghosh MC, Ollivierre W, Weitzel RP, Eckhaus MA, et al. (2014) Wild-type macrophages reverse disease in heme oxygenase 1-deficient mice. Blood 124: 1522-1530.

13 Tafazoli S, Spehar DD, Brien PJO (2005) Oxidative stress mediated idiosyncratic drug toxicity. Drug Metab Rev 37: 311-325.

14 Kim TH, Yoon SJ, Lee SM (2012) Genipin attenuates sepsis by inhibiting Toll-like receptor signaling. Mol Med 18: 455-465.

15 Chistyakov VA, Smirnova YO, Prazdnova EV, Soldatov AV (2013) Possible mechanisms of fullerene C(6)(0) antioxidant action. Biomed Res Int 2: 1-4.

16 Katsumi H, Fukui K, Sato K, Maruyama S, Yamashita S, et al. (2014) Pharmacokinetics and preventive effects of platinum nanoparticles as reactive oxygen species scavengers on hepatic ischemia/reperfusion injury in mice. Metallomics 6: 1050-1056.

17 Yang X, Jin L, Yao L, Shen FH, Shimer AL, et al. (2014) Antioxidative nanofullerol prevents intervertebral disk degeneration. Int J Nanomedicine 9: 2419-2430.

18 Wang C, Blough E, Dai X, Olajide O, Driscoll H, et al. (2016) Protective Effects of Cerium Oxide Nanoparticles on MC3T3-E1 Osteoblastic Cells Exposed to X-Ray Irradiation. Cell Physiol Biochem 38: 1510-1519.

19 Chen S, Hou Y, Cheng G, Zhang C, Wang S, et al. (2013) Cerium oxide nanoparticles protect endothelial cells from apoptosis induced by oxidative stress. Biol Trace Elem Res 154: 156-166.

20 Chaudhury K, Babu N, Singh AK, Das S, Kumar A, et al. (2013) Mitigation of endometriosis using regenerative cerium oxide nanoparticles. Nanomedicine 9: 439-448.

21 Kyosseva SV, Chen L, Seal S, McGinnis JF (2013) Nanoceria inhibit expression of genes associated with inflammation and angiogenesis in the retina of Vldlr null mice. Exp Eye Res 116: 63-74.

22 Lee SS, Song W, Cho M, Puppala HL, Nguyen P, et al. (2013) Antioxidant properties of cerium oxide nanocrystals as a function of nanocrystal diameter and surface coating. ACS Nano 7: 9693-703.

23 Clark A, Zhu A, Sun K, Petty HR Cerium (2011) oxide and platinum nanoparticles protect cells from oxidant-mediated apoptosis. J Nanopart Res 13: 5547-5555.

24 Pirmohamed T, Dowding JM, Singh S, Wasserman B, Heckert E, et al. (2010) Nanoceria exhibit redox state-dependent catalase mimetic activity. Chem Commun (Camb) 46: 2736-2738.

25 Claessens YE, Dhainaut JF (2007) Diagnosis and treatment of severe sepsis. Crit Care 5: S2.

26 Selvaraj V, Nepal N, Rogers S, Manne ND, Arvapalli R, et al. (2015) Inhibition of MAP kinase/NF-kB mediated signaling and attenuation of lipopolysaccharide induced severe sepsis by cerium oxide nanoparticles. Biomaterials 59: 160-171.

27 Nalabotu SK, Kolli MB, Triest WE, Ma JY, Manne ND, et al. (2011) Intratracheal instillation of cerium oxide nanoparticles induces hepatic toxicity in male Sprague-Dawley rats. Int J Nanomedicine 6: 2327-2335.

28 Wang Y, Wu M, Al Rousan R, Liu H, Fannin J, et al. (2011) Iron-induced cardiac damage: role of apoptosis and deferasirox intervention. J Pharmacol Exp Ther 336: 56-63.

29 Hillegass LM, Griswold DE, Brickson B, Albrightson-Winslow C (1990) Assessment of myeloperoxidase activity in whole rat kidney. J Pharmacol Methods 24: 285-295.

30 Wang F, Fu X, Wu X, Zhang J, Zhu J, et al. (2018) Bone marrow derived M2 macrophages protected against lipopolysaccharide-induced acute lung injury through inhibiting oxidative stress and inflammation by modulating neutrophils and T lymphocytes responses. Int Immunopharmacol 61: 162-168.

31 Zarbock A, Gomez H, Kellum JA (2014) Sepsis-induced acute kidney injury revisited: pathophysiology, prevention and future therapies. Curr Opin Crit Care 20: 588-595.

32 Lindell RB, Gertz SJ, Rowan CM, McArthur J, Beske F, et al. (2017) High Levels of Morbidity and Mortality Among Pediatric Hematopoietic Cell Transplant Recipients with Severe Sepsis: Insights from the Sepsis PRevalence, OUtcomes, and Therapies International Point Prevalence Study. Pediatr Crit Care Med 18: 1114-1125.

33 Wu L, Gokden N, Mayeux PR (2007) Evidence for the role of reactive nitrogen species in polymicrobial sepsis-induced renal peritubular capillary dysfunction and tubular injury. J Am Soc Nephrol 18: 1807-1815.

34 Vaidya VS, Ferguson MA, Bonventre JV (2008) Biomarkers of acute kidney injury. Annu Rev Pharmacol Toxicol 48: 463-493.

35 Bosmann M, Ward PA (2013) The inflammatory response in sepsis. Trends Immunol 34: 129-136.

36 Hirst SM, Karakoti A, Singh S, Self W, Tyler R, et al. (2013) Bio-distribution and in vivo antioxidant effects of cerium oxide nanoparticles in mice. Environ Toxicol 28: 107-118.

37 Wang C, Wu M, Arvapalli R, Dai X, Mahmood M, et al. (2014) Acetaminophen attenuates obesity-related renal injury through ER-mediated stress mechanisms. Cell Physiol Biochem 33: 1139-1348.

38 Cui WY, Tian AY, Bai T (2011) Protective effects of propofol on endotoxemia-induced acute kidney injury in rats. Clin Exp Pharmacol Physiol 38: 747-754.

39 Cross LJ, Matthay MA (2011) Biomarkers in acute lung injury: insights into the pathogenesis of acute lung injury. Crit Care Clin 27: 355-377.

40 Zhao YY, Gao XP, Zhao YD, Mirza MK, Frey RS, et al. (2006) Endothelial

cell-restricted disruption of FoxM1 impairs endothelial repair following LPS-induced vascular injury. J Clin Invest 116: 2333-2343.

41 Wang G, Huang X, Li Y, Guo K, Ning P, et al. (2013) PARP-1 inhibitor, DPQ, attenuates LPS-induced acute lung injury through inhibiting NF-kappaB-mediated inflammatory response. PLoS One 8: e79757.

42 Hoth JJ, Wells JD, Hiltbold EM, McCall CE, Yoza BK (2011) Mechanism of neutrophil recruitment to the lung after pulmonary contusion. Shock 35: 604-609.

43 Martin TR, Mathison JC, Tobias PS, Leturcq DJ, Moriarty AM, et al. (1992) Lipopolysaccharide binding protein enhances the responsiveness of alveolar macrophages to bacterial lipopolysaccharide. Implications for cytokine production in normal and injured lungs. J Clin Invest 90: 2209-2219.

44 Yingkun N, Zhenyu W, Jing L, Xiuyun L, Huimin Y (2013) Stevioside protects LPS-induced acute lung injury in mice. Inflammation 36: 242-250.